

Translational activity of 80S monosomes varies dramatically across different tissues

Albert Blandy^{1,2,3,†}, Tayah Hopes^{1,2,3,†}, Elton J.R. Vasconcelos^{1,2}, Amy Turner^{1,3},
Bulat Fatkhullin^{1,3}, Michaela Agapiou^{1,2}, Juan Fontana^{1,3,4,*}, Julie L. Aspden^{1,2,3,*}

¹School of Molecular and Cellular Biology, Faculty of Biological Sciences, University of Leeds, LS2 9JT, UK

²LeedsOmics, University of Leeds, Leeds, LS2 9JT, UK

³Astbury Centre for Structural Molecular Biology, University of Leeds, Leeds, LS2 9JT, UK

⁴Present address: Instituto Biofisika, CSIC-UPV/EHU, Barrio Sarriena s/n, Leioa, Bizkaia, Spain

*To whom correspondence should be addressed. Email: j.aspden@leeds.ac.uk

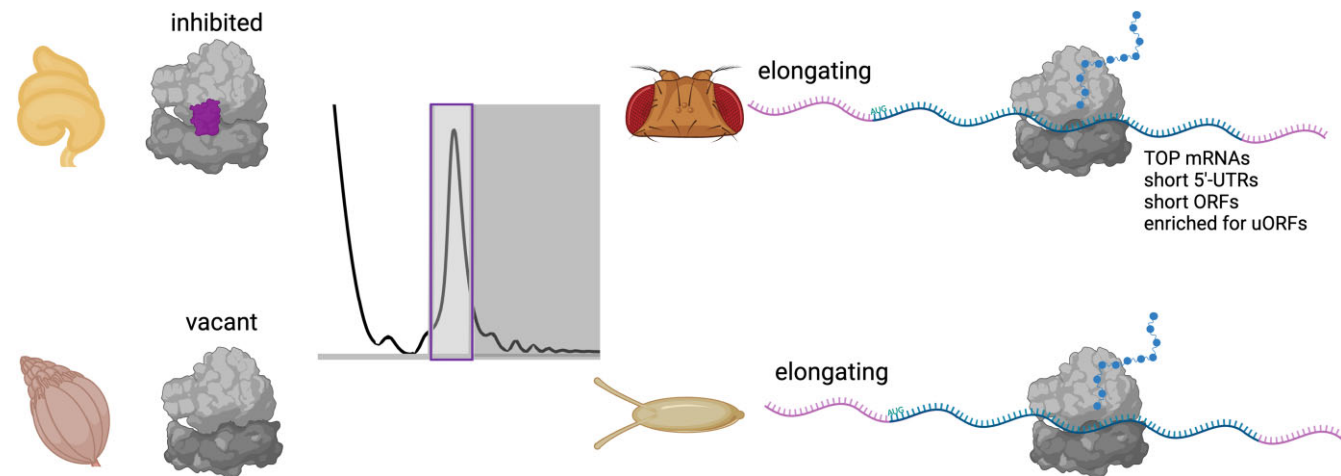
Correspondence may also be addressed to Juan Fontana. Email: juan.fontana@csic.es

†These authors contributed equally.

Abstract

Translational regulation at the stage of initiation can impact the number of ribosomes translating each mRNA molecule. However, the translational activity of single 80S ribosomes (monosomes) on mRNA is less well understood, even though these 80S monosomes represent the dominant ribosomal complexes *in vivo*. Here, we used cryo-EM to determine the translational activity of 80S monosomes across different tissues in *Drosophila melanogaster*. We discovered that while head and embryo 80S monosomes are highly translationally active, testis and ovary 80S monosomes are translationally inactive. RNA-Seq analysis of head monosome- and polysome-translated mRNAs, revealed that head 80S monosomes preferentially translate mRNAs with TOP motifs, short 5'-UTRs, short ORFs and are enriched for the presence of uORFs. Overall, these findings highlight that regulation of translation initiation and protein synthesis is mostly performed by monosomes in head and embryo, while polysomes are the main source of protein production in testis and ovary.

Graphical abstract



Introduction

Translation levels are tightly regulated during development and differentiation across eukaryotes [1]. Much of this control acts during the initiation of protein synthesis, regulating the rate of 80S formation and, therefore, the number of ribosomes bound per mRNA [2]. mRNAs bound by many ribosomes are termed poly-ribosomes or polysomes [3]. The binding of multiple ribosomes on a single mRNA facilitates efficient protein synthesis; therefore, there is a generally held assumption that mRNAs bound by 80S monosomes are less translated than

those bound by polysomes. However, several factors complicate this simple assumption, including the length of an ORF and therefore the space available to be bound by multiple ribosomes at the same time [4–6].

The proportion of ribosomes engaged as 80S monosomes or polysomes varies across cell types, tissues, and response to stimuli (e.g. during differentiation [7]). Measuring translation, its regulation and how this differs across cells can be achieved by numerous techniques. The most widely used approach to assess translation levels and how they change, is

Received: July 15, 2024. Revised: March 23, 2025. Editorial Decision: March 24, 2025. Accepted: May 2, 2025

© The Author(s) 2025. Published by Oxford University Press on behalf of Nucleic Acids Research.

This is an Open Access article distributed under the terms of the Creative Commons Attribution License (<https://creativecommons.org/licenses/by/4.0/>), which permits unrestricted reuse, distribution, and reproduction in any medium, provided the original work is properly cited.

polysome profiling [8]. This involves the separation of ribosomal complexes in sucrose gradients on the basis of the number of ribosomes bound per mRNA, providing an overview of the translational status of a sample. The distribution of individual mRNAs can then be assessed across the gradient to measure what proportion of the mRNA is bound by ribonucleoproteins, 40S subunits, 80S monosomes and polysomes [7].

It has been a long-standing assumption that single 80S monosomes consist of two types of ribosomes: (i) inactive “vacant” 80S, not engaged on mRNAs [9]; and (ii) translationally active 80S, which could be initiating, elongating, or terminating. However, the relative proportions of these two types of 80S has not been determined. Dissecting the translational capability of different sized translational complexes, i.e. 80S monosomes versus small polysomes versus large polysomes, has important consequences on understanding rates of protein synthesis and translational regulation. For example, it has previously been shown that in neuronal axons and dendrites, 80S monosomes are highly translationally active and represent a substantial part of the protein synthesis machinery [10]. Additionally, ribosome profiling of yeast 80S monosomes has shown that most of them are engaged in elongation rather than initiation [4]. “Vacant” ribosomes, not engaged in translation, have been shown in several systems to be bound by factors within the mRNA channel preventing mRNA binding. This includes prokaryotic hibernation factors [11] and eukaryotic dormancy factors, which stabilise 40S and 60S binding to form 80S monosomes, and prevent 40S binding to mRNAs, allowing for regulation during stress or development [12, 13].

This study set out to determine what proportion of 80S ribosomes are engaged in active translation in *Drosophila melanogaster* (*D. melanogaster*) tissues, and if tissue-specific differences exist. This has revealed a stark difference between translation states of 80S monosomes between tissues. We also found that within heads, 80S monosomes and polysomes translated different mRNA pools, with distinct molecular characteristics and encoding specific protein functions.

Together this work shows that protein synthesis in the *Drosophila* head and embryo is mostly performed by monosomes, in contrast to testis and ovary, where polysomes are the main source of protein production.

Materials and methods

Fly husbandry and stocks

Flies were kept in a 25°C humidified room with a 12:12 h light:dark cycle and raised on standard sugar-yeast-agar medium in 6 oz Square Bottom Bottles (Flystuff).

Tissue harvest for cryo-EM and RNA-seq

Around 5 mL of 0–5 day old whole flies were snap frozen in liquid nitrogen (LN₂) and subjected to mechanical shock to detach heads. Heads were isolated by passing through a 1 mm mesh filter with LN₂. 1.5 g of embryos were collected at 0–2 h from laying plates [300 mL grape juice concentrate (Young’s Brew), 25 g agar, 550 mL dH₂O, 10% nipagin]. Laying plates were scored and applied with yeast paste consisting of active dried yeast (DCL), plates were placed in cages after pre-clearing for 2 h. Embryos were transferred to 70 mm mesh filter, washed with dH₂O, dried and flash frozen in LN₂. 500–

1000 pairs of testes were harvested from 1- to 4-day-old males in 1 × PBS with 2 mM DTT and 1 U/μl RNAsin Plus and flash frozen in LN₂ [14]. Approximately 300 pairs of ovaries were dissected from 3 to 6-day-old females in 1 × PBS (Lonza) with 1 mM DTT (Sigma) and 1 U/μl RNAsin Plus (Promega) and flash frozen in LN₂ [14].

Ribosome purification for cryo-EM and RNA-seq

All stages of ribosome purification were performed on wet ice or at 4°C, wherever possible. Heads were transferred to an 8 mL glass Dounce with 1.5 mL lysis buffer A [10 mM Tris-HCl pH 7.5, 150 mM NaCl, 10 mM MgCl₂ (Fluka), 1% IGEPAL CA-630 (Sigma), 1% Triton X-100, 0.5% sodium deoxycholate (Sigma), 2 mM DTT, 200 μg/mL cycloheximide, 2 U/mL Turbo DNase (Thermo Fisher), 40 U/mL RNAsin Plus, 1 × EDTA-free protease inhibitor cocktail (Roche), 0.5% DOC] per gradient. Embryos were ground with a pre-chilled pestle and mortar in LN₂ and incubated with 1.5 mL lysis buffer A per gradient. Ovaries and testes were ground using RNase-free 1.5 mL pestles (SLS) in 500 mL lysis buffer B per gradient [50 mM Tris-HCl pH 8 (Sigma), 150 mM NaCl, 10 mM MgCl₂, 1% IGEPAL CA-630, 1 mM DTT, 100 μg/mL cycloheximide, 2 U/μL Turbo DNase, 0.2 U/μL RNAsin Plus, 1 × EDTA-free protease inhibitor cocktail] [14]. All samples were incubated for 30 min with occasional agitation. To obtain the cytoplasmic lysate, both head and embryo preparations were centrifuged to remove cell debris and floating fat at 17 000 × g for 10 min.

Cytoplasmic lysates were loaded onto a 18–60% (w/v) sucrose gradient [50 mM Tris-HCl pH 8.0, 150 mM NaCl, 10 mM MgCl₂, 100 mg/mL cycloheximide, 1 mM DTT, 1 × EDTA-free protease inhibitor cocktail (Roche)] and ultracentrifuged for 3.5 h at 170 920 × g at 4°C. Fractions were collected using a Gradient StationBiocomp equipped with a fraction collector (Gilson) and Econo UV monitor (BioRad). Fractions corresponding to either monosomes or polysomes were combined. These fractions were concentrated using 30 kDa column (Amicon Ultra-4 or Ultra-15) at 4°C and buffer exchanged (50 mM Tris-HCl pH 8, 150 mM NaCl, 10 mM MgCl₂) until final sucrose ≤ 0.1%. The foot-printed 80S polysomes were isolated from pooled polysomal fractions of the embryo extract ribosome purification sucrose gradient and treated with RNaseI (4 U/area under the curve; AUC at 254 nm at 4°C overnight. SuperRNAsin was added for 5 min at 4°C, preventing over digestion of mRNA. A second ribosome purification step was carried out on this sample, isolating the 80S fractions. Fractions were pooled and diluted to <0.1% sucrose and concentrated using Amicon Ultra-4 centrifugal filter units (MWCO 30 kDa) to > 200 nM. Samples were quantified using Qubit Protein Assay Kit (Invitrogen) [14].

Application to cryo-EM grids

Purified ribosomes were diluted as required with dilution buffer (50 mM Tris-HCl pH 8.0, 150 mM NaCl, 10 mM MgCl₂). Copper grids covered with a lacey carbon and an ultrathin layer of carbon (Agar Scientific) were glow discharged for 30 s (easiGlow, Ted Pella), and 3 μL of purified ribosomes were added to the grid surface in a chamber at 4°C and 95% humidity conditions. Sample excess was blotted and grids were vitrified by plunge-freezing in liquid ethane cooled by liquid nitrogen using an EM GP plunge freezer (Leica) [14].

Cryo-EM data collection

For all samples, cryo-EM data collection was carried out using FEI Titan Krios (Thermo Fisher) transmission electron microscope with an accelerating voltage of 300 keV. Data was recorded on a Falcon III direct electron detector in integrating mode at a pixel size of 1.065 Å. The total number of collected micrographs for the head 80S monosomes was 14 827, while for the foot-printed testis polysomes, a total of 8128 micrographs were collected. For both samples, a total electron dose of 82 e⁻/Å² partitioned into a dose of 1.37 e⁻/Å² per fraction (60 fractions) was employed. Data collections for all other samples have been described previously [14].

Cryo-EM image processing

Cryo-EM image processing was performed as previously described [15, 16]. Motion correction and CTF estimation were performed using MOTIONCORR and gCTF, respectively [17, 18]. For the head 80S monosomes 735 663 particles were picked using crYOLO's general model [19]. For the testis foot-printed polysomes, autopicking was performed in Relion, resulting in 185 095 particles. Relion was used for further processing. 2 rounds of reference free 2D classification were used to align and classify autopicked particles into 200 classes. 2D classifications were used to iteratively remove “junk” particles selected from autopicking. After both rounds of 2D classification, the head 80S dataset resulted in 610 605 particles while the embryo footprinted polysomes dataset resulted in 69 712 particles. The previously produced *D. melanogaster* testis 80S ribosome average was used as a reference average for 3D classification [14]. These particles were further 3D classified, refined, and postprocessed, resulting in averages at a final resolution of 3.0 Å for the heads 80S dataset (Supplement Fig. S2) and of 4.7 Å for the embryo footprinted polysomes.

Focused classification

The proportion of 80S monosomes and polysomes engaged in active translation in the *D. melanogaster* head, embryo, testis, and ovary tissues was determined by tRNA occupation assessment by focused classification of the different datasets. The head 80S monosome dataset contained 610 605 particles (as above), the embryo 80S monosome dataset 11 446 particles, the embryo foot-printed 80S polysome dataset 34 603 particles, the testis 80S monosome dataset 46 878 particles, the testis 80S polysome dataset 10 392 particles and the ovary 80S monosome dataset 185 913 particles. After 3D refinement carried out using unbinned particles, as described above, particles were then binned five times to expedite image processing (5.325 Å pixel size), given that tRNAs are easily distinguished at the theoretical maximum resolution achievable (10.65 Å).

A mask around the mRNA channel was then generated, and a 10-class 3D classification without alignment was performed. To resolve the full 80S monosome structure while maintaining the structural detail from the masked focused classification, a final unmasked reconstruction of each class was performed. This allowed imaging the full 80S monosome, aiding orientating, and assessing the mRNA channel and tRNA positions in the context of the whole 80S monosome.

tRNA and IFRD1 atomic model fitting

To determine the conformation of tRNAs in the *D. melanogaster* tissue ribosomes, reference eukaryotic tRNA

atomic models were chosen from variety of organisms, as only the P/P and E/E tRNAs are currently available from *D. melanogaster* ribosome atomic models. These included the A/A tRNA from *S. cerevisiae* (PDB 5GAK), the A/P and P/E tRNAs from rabbit reticulocyte lysate (PDB 6HCJ) and P/P and E/E tRNAs from *D. melanogaster* (respectively, PDB 6XU7 and 4V6W). The IFRD1 atomic model was selected from the *D. melanogaster* testis 80S monosome atomic model (PDB 6XU6) [14].

RNA-seq

Head tissue was harvested, and ribosomes were purified as above [14]. 10% of cell lysate was retained for sequencing total RNA. Fractions were isopropanol-precipitated (1 vol isopropanol, 300 mM NaCl final) overnight at -80°C, then centrifuged at 17 000 x g for 20 min and washed in 70% ethanol. 80S monosome fractions were combined, as were polysome fractions. Total RNA and sucrose gradient fractions were treated with TURBO DNase (Ambion) and purified using Quick-RNA Microprep Kit (Zymo). Samples were rRNA depleted with QIAseq FastSelect -rRNA Fly Kit (QIAGEN). Sequencing libraries were prepared with the TruSeq Stranded mRNA kit (Illumina) and run on the NextSeq 2000, 100 cycle lane (Illumina).

RNA-seq analysis

RNA single-read sequencing quality control was assessed through FastQC (www.bioinformatics.babraham.ac.uk/projects/fastqc) and multiQC [20]. An average of 45 million reads were sequenced per sample. Both adapters and low-quality bases (QV < 20) were trimmed from reads' extremities using Trimmomatic [21] with a minimum read length of 25 bp. All libraries were mapped against the *D. melanogaster* BDGP6.32 release-109 reference genome (http://ftp.ensembl.org/pub/release-109/fasta/drosophila_melanogaster/dna/Drosophila_melanogaster.BDGP6.32.dna.toplevel.fa.gz) through STAR aligner [22] with default parameters. STAR-generated sorted BAM output files were used for assigning read counts to gene features with featureCounts [23] with the following parameters: -M -O -fraction -s 2. *Drosophila_melanogaster*.BDGP6.32.109.gtf annotation file from ensembl was used.

Read counts table generated by featureCounts was then used as input for DE analyses relying on the DESeq2 negative binomial distribution model through a local fitting type and a 0.01 FDR threshold [24]. DE pairwise comparisons were performed as 80S-vs-Polysomes, Total-vs-80S, and Total-vs-Polysomes, being the second term the numerator in the fold-change ratio. EnhancedVolcano (<https://bioconductor.org/packages/release/bioc/html/EnhancedVolcano.html>) was employed for an overall DE visualisation through volcano plots. GO- and KEGG-based gene enrichment analyses for individual DEGs lists were performed by clusterProfiler Bioconductor package [25] under R v4.1.0, setting adjusted *P*-value < 0.05. Both 5'- and 3'-UTRs were extracted from *Drosophila_melanogaster*.BDGP6.32.109.gtf. An empirical cumulative distribution function plus Kolmogorov-Smirnov Tests were run within the R v4.1.0 environment to assign significance to UTR lengths comparison between conditional groups (80S, Polysomes, and Total RNA). STREME from the MEME suite v5.4.1 [26] was employed for motif screening within the UTRs of both 80S- and Polysome-enriched

transcripts under the following parameters: `-rna -minw 5 -maxw 15 -thresh 0.01`. A negative control set of randomly-selected non-DEGs' UTRs in the same amount of the DEGs' ones was used for the `-n` option. A list of uORFs-containing transcripts was retrieved from [27] and then mapped against both 80S and Polysome DEGs' list for building a 2×2 contingency table and running a Fisher Exact Test. The generalised boosted models (gbm) R package (<https://github.com/gbm-developers/gbm>) was employed through an *ad-hoc* R script (kindly provided by Dr Tobias Schmidt and Dr Joseph Waldron https://github.com/Bushell-lab/Ribo-seq/blob/main/R_scripts/feature_properties/gradient_boosting.R) to infer the relative influence of certain gene features (e.g. uORF presence, UTRs and CDSs lengths, %GC and %GA) on the Polysome/80S DE ratio (\log_2 FC).

KCl treatment

For heads, 1–5 day-old flies were sedated using ice. On an iced glass petridish, 50 heads were removed and placed in 173 μ L dissecting buffer (Schneider's media with x1 EDTA-free protease inhibitor cocktail (Roche), x1 RNasin Plus (Promega) and 100 μ g/mL cycloheximide). This was repeated to 150 heads per gradient. For ovaries and testis, 1–5 day-old flies were sedated using ice. On a dissecting dish, 20 ovaries were removed and placed in 173 μ L dissecting buffer. On a dissecting dish, 150 testis were dissected in Ringers solution supplemented with x1 RNasin Plus (Promega) and EDTA-free protease inhibitor cocktail (Roche) and flash frozen (10 pairs at a time). Heads, ovaries and testis were ground using RNase-free 1.5 mL pestles (SLS). Around 207 μ L lysis buffer A plus 100 or 200 mM KCl. Samples were lysed on ice for ≥ 30 min, then centrifuged at 17 000 \times g for 10 min at 4°C.

Linear 15–50% (w/v) sucrose gradients were made using a Gradient StationBioComp. Sucrose was supplemented with 50 mM Tris-KCl pH 8.0, 150 mM NaCl, 10 mM MgCl₂, 100 mg/mL cycloheximide, 1 mM DTT, 1 \times EDTA-free Protease Inhibitor cocktail (Roche), and 0, 100 mM or 200 mM KCl. 1 mL of sucrose was removed from the top of the gradient and 500 μ L of cytoplasmic lysates were loaded to the top of the gradient. Gradients were ultra-centrifuged in an SW40Ti rotor (Beckman) for 4:15 h at 170 920 \times g at 4°C and fractionated as above.

Puromycin assays

To obtain tissue, flies were sedated by cooling in small batches to minimise time between sedation and puromycin assay. Twenty-eight heads per replicate were harvested on an iced petri dish. Forty-nine pairs of testis and 3.5 pairs ovaries per replicate were harvested into Ringer's solution on a dissecting dish. This is equivalent to 4 heads, 7 pairs testis and 0.5 pairs ovary per time point. All tissues were dissected into a 1.5 mL Eppendorf containing 56 μ L room temperature Schneiders buffer supplemented with RNasin Plus (Promega) and EDTA-free protease inhibitor cocktail (Roche). Tissue was lysed with a micropestle, briefly centrifuged to remove debris and aliquoted in 4 \times 8 μ L. Puromycinylation was initiated with 50 μ g/mL puromycin and 40 μ M emetine and stopped with 200 μ g/ μ L cycloheximide after 1, 5, or 15 min, then placed on ice. The puromycin negative control was treated with cycloheximide and kept on ice. Protein sample loading buffer was added to the samples before heating to 95°C for 2 min and subsequent benzonase treatment (Merk; 0.2 μ L for

5 min at 37°C). After SDS-PAGE and transfer, the revert total protein stain (LI-COR) was performed. Membranes were then blocked in 5% milk + TBS for 1 h. Mouse anti-puromycin (company, cat no) in 5% milk + TBST was applied for 1 h, at room temperature, 1:1000. Goat anti-mouse Alexa Flour 680 secondary was applied at 1:10 000 in TBST for 1 h, at room temperature and protected from light. All images were obtained using the LI-COR Odyssey M scanner and analysed using LI-COR ImageStudio.

Data availability

GEO GSE267425 <https://www.ncbi.nlm.nih.gov/geo/query/acc.cgi?acc=GSE267425>.

Results

Cryo-EM of 80S ribosomes from *D. melanogaster* heads at 3.0 Å

To profile the translational activity across different tissues we purified ribosomes from *D. melanogaster* heads, 0–2 h embryos, testes and ovaries. As we have previously shown, the sucrose gradient profiles from these tissues vary in their precise ratio of 80S monosomes to polysomes [14]. However, what is in common between these tissues is that the majority of ribosomes present are 80S monosomes (Supplement Fig. S1), while the minority are polysomes, in contrast to *D. melanogaster* S2 tissue culture cells [5, 14]. Therefore, we sought to understand whether these 80S monosomes were in fact involved in active translation and if this varies across tissues. Cryo-EM was performed on 80S monosomes from heads and a dataset containing ~600 000 particles was collected. Image processing of this head 80S dataset as a single class was refined to an average 3.0 Å resolution (Supplementary Fig. S2A).

In contrast to the previous structures that we had determined for testis 80S and ovary 80S monosomes, which contained no tRNA [14], the head 80S map contained tRNAs in A/A and P/P sites, and to a lesser extent the P/E site, which we interpreted as evidence of multiple classes present in the sample. tRNA sites are classified according to their position in 40S/60S subunits within the 80S ribosome, reflecting the positions of tRNA during the elongation cycle. P/E is a hybrid state where tRNA is in P site of 40S and E site of 60S. This indicates that the majority of the head 80S monosome are likely engaged in elongation, and therefore actively translating.

The vast majority of head 80S monosomes contain tRNAs

To dissect the tRNA occupancy of the head 80S monosomes more precisely, we performed focused classification around the mRNA channel and A/P/E tRNA sites of the head 80S 3D average. To ensure potential classes were not limited by the image processing workflow, we attempted classification into 10 classes. This resulted in six significant classes (which we defined as containing >1% of the dataset particles and >200 particles) from the head 80S monosome dataset (Fig. 1A–F, Supplement Table S1). Five of six of these classes contained tRNAs occupying various sites within the mRNA channel, reflective of different states during translation elongation. Quantification of the number of particles contributing to these classes revealed that ~61% head 80S monosomes had tRNAs in A/A and P/P sites (Fig. 1A–C), ~19% in P/E and A/P sites

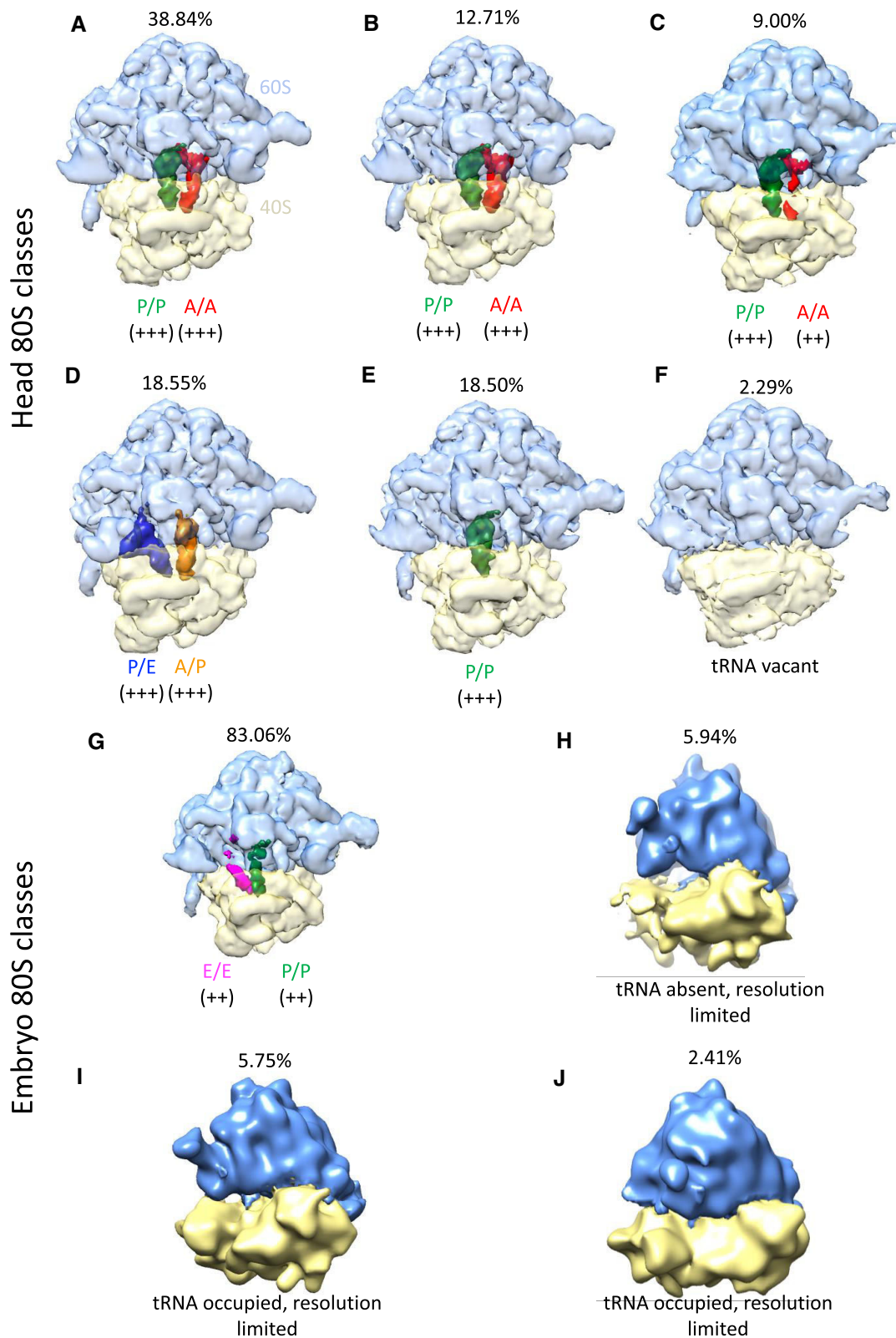


Figure 1. 80S monosomes from *D. melanogaster* head and embryo are actively translating. Significant 3D classes (>1% total particles in dataset and >300 particles) of the head 80S dataset (A–F) from ~600 000 particles; and 0–2 h embryo 80S monosome dataset (G–J) from ~11 500 particles. (A–C) 3 classes of the head 80S dataset, representing 38.84%, 12.71%, and 9.00% of the head 80S particles, contained tRNA densities in P/P and A/A sites. (D) Around 18.55% of the head 80S particles (1 class) contained tRNA densities in P/E and A/P sites. (E) Around 18.50% of head 80S particles (1 class) contained tRNA densities in P/P sites. (F) Around 2.29% head 80S particles were tRNA vacant. (G) Around 83.06% of the embryo 80S particles (1 class) contained tRNA densities in E/E and P/P sites. (H) Around 5.94% of embryo 80S particles (1 class) were tRNA vacant. (I and J) Two classes, representing 5.75% embryo and 2.41% of embryo 80S particles, contained densities within the mRNA channel and therefore are tRNA occupied, but resolution is limited. Percentage of particles in each class is given above each class. tRNA site positions are indicated along with score of confidence with ++ medium confidence and +++ highly confident.

(Fig. 1D) and ~19% in P/P alone (Fig. 1E). Only ~2% of the ribosomes had no tRNAs present (Fig. 1F).

Additionally, we generated a second cryo-EM head 80S monosomes data set from a biological replicate, which contained ~7700 particles. The focused classification of the mRNA channel and tRNA sites of this sample generated two major classes, both with tRNAs present: ~52% in the A/P and P/E sites and ~47% in the P/P site (Supplementary Fig. S2B and C, Supplement Table S1). Overall, this analysis indicates that ~98–99% of 80S monosomes are engaged in active translation in the head.

Most 80S monosomes from embryo exhibit tRNA occupancy

To profile the translational activity in the same way for embryo 80S monosomes we performed cryo-EM on 80S monosomes purified from 0 to 2 h embryos and a dataset containing ~11 500 particles was collected. Image processing of this embryo 80S dataset resulted in an average at 5.4 Å resolution. We again performed focused classification around the mRNA channel and tRNA sites, resulting in four significant classes. Although fewer particles were contributing to this dataset meant some classes were resolution limited, we could still determine whether they were tRNA occupied or absent (Fig. 1G–J).

Like in the head, the vast majority (~91%) of these embryo 80S monosomes contained tRNA, reflective of active translation elongation (Fig. 1G, I, and J, Supplementary Table S1). The main tRNA occupied state detected in embryo converged into a single class that contained densities for E/E and P/P tRNAs. Together with the head results, this confirms that monosomes can be actively engaged in translation in specific tissues, in contrast to the large abundance of polysomes present in tissue cultured cells.

No monosomes are engaged in active translation in ovaries or testes

The averages we had previously generated for testis and ovary 80S monosomes did not contain tRNAs [14]. These datasets consisted of ~47 000 and ~186 000 particles respectively, which resulted in cryo-EM averages at 3.5 and 3.0 Å resolution. However, no focused classification around the mRNA channel/tRNA sites was performed on these datasets. To determine if small proportions of particles did contain tRNAs, and therefore were actively translating, we performed focused classification and quantification on these datasets. We were unable to detect any testis 80S monosomes with tRNAs present. Instead, two significant classes were identified, both with the mRNA channel occupied by interferon-related developmental regulator 1 (IFRD1) (Fig. 2A and B). Building on our previous work showing the presence of IFRD1 (Hopes *et al.*, 2022), this analysis revealed that all 80S monosomes in the testis are inactive, inhibited by the presence of IFRD1. The mammalian ortholog, IFRD2, has a role in translational regulation during differentiation and was detected in P- and E- sites of ~20% 80S ribosomes isolated from rabbit reticulocytes [13]. Additionally, all four significant classes of ovary 80S monosomes had empty mRNA channels, with no tRNA density present (Fig. 2C–F, Supplement Table S1). Together, this analysis reveals that virtually no testis or ovary 80S monosomes are actively translating.

Ribosome complexes derived from polysomes are actively engaged in translation

As a positive control, we also performed mRNA channel focused classification on 2 samples expected to be highly active in translation: a) testis polysomes and b) 80S ribosomes derived from foot-printed embryo polysomes. These datasets contained ~10 000 and ~34 500 particles, respectively, and resulted in averages at 4.9 and 4.7 Å resolution. Over 97% of testis polysomes were tRNA occupied and therefore engaged in translation, exhibiting tRNA in the P/P and A/A sites (Supplementary Fig. S3A, Supplementary Table S1). Similarly, RNaseI footprinted polysomes from 0 to 2 h embryos resulted in 4 significant classes, all of which were tRNA occupied and included P/E and A/P sites, E/E and P/P sites, and P/P and A/A sites (Supplementary Fig. S3B–E).

Overall, this analysis revealed that there is a clear contrast in the translational activity of 80S monosomes across different tissues (Fig. 3, Supplementary Table S2). Head and embryo 80S monosomes are highly translationally active, testis 80S monosomes are inhibited, and ovary 80S monosomes are vacant. As expected polysomal ribosomes are actively translating. The extent of 80S monosome vacancy is unlikely to be the result of difference in elongation rates, since puromycin time course assays revealed there is no statistical difference in elongation rate between head and either ovary or testis (Supplementary Fig. S4).

Translating 80S monosomes are stable in high salt conditions

To characterise the 80S monosomes in more detail we assessed their sensitivity to high KCl. Most ribosome purification buffers contain 0–100 mM KCl [28, 29], but high KCl (e.g. 200 mM) has been shown to dissociate vacant ribosomes not engaged with mRNAs [30–32]. Therefore, to biochemically confirm that most 80S monosomes from heads are translating and therefore bound to mRNAs, we treated head, ovary, and testis 80S monosomes with increasing concentrations of KCl (0, 100, and 200 mM) and monitored the effects of the incubation using sucrose gradients (Fig. 4, Supplementary Fig. S5). At 0 mM all samples contain a large amount of 80S monosomes. At 100 mM KCl, which is widely used in sucrose gradient analysis, the majority of head 80S remain associated (Fig. 4A, Supplementary Fig. S5A, 0 and 100 mM KCl), while some 80S ovary monosomes disassociate. At this concentration some testis 80S monosomes also dissociate, even though they are bound by IFRD1 (Supplementary Figs S5 and S6). At 200 mM KCl vast the majority of head ribosomes remained as 80S monosomes (Fig. 4A, Supplementary Fig. S5A and B, 200 mM), while the majority (~90%) of ovary 80S monosomes were disassociated into 40S and 60S subunits (Fig. 4B, Supplementary Fig. S5, 200 mM and S6). Although a higher proportion of testis 80S monosomes disassociate at 200 mM KCl compared to 100 mM, ~50% remain as 80S (Fig. 4C, Supplementary Figs S5C, S6, 200 mM). The observation that head 80S monosomes are mostly insensitive to KCl, but the majority of ovary 80S monosomes are sensitive, supports the conclusion that most head 80S monosomes are translating, while most ovary 80S monosomes are vacant. Testis 80S monosomes are less sensitive to higher KCl than ovary 80S, likely due to stabilisation by IFRD1 binding.

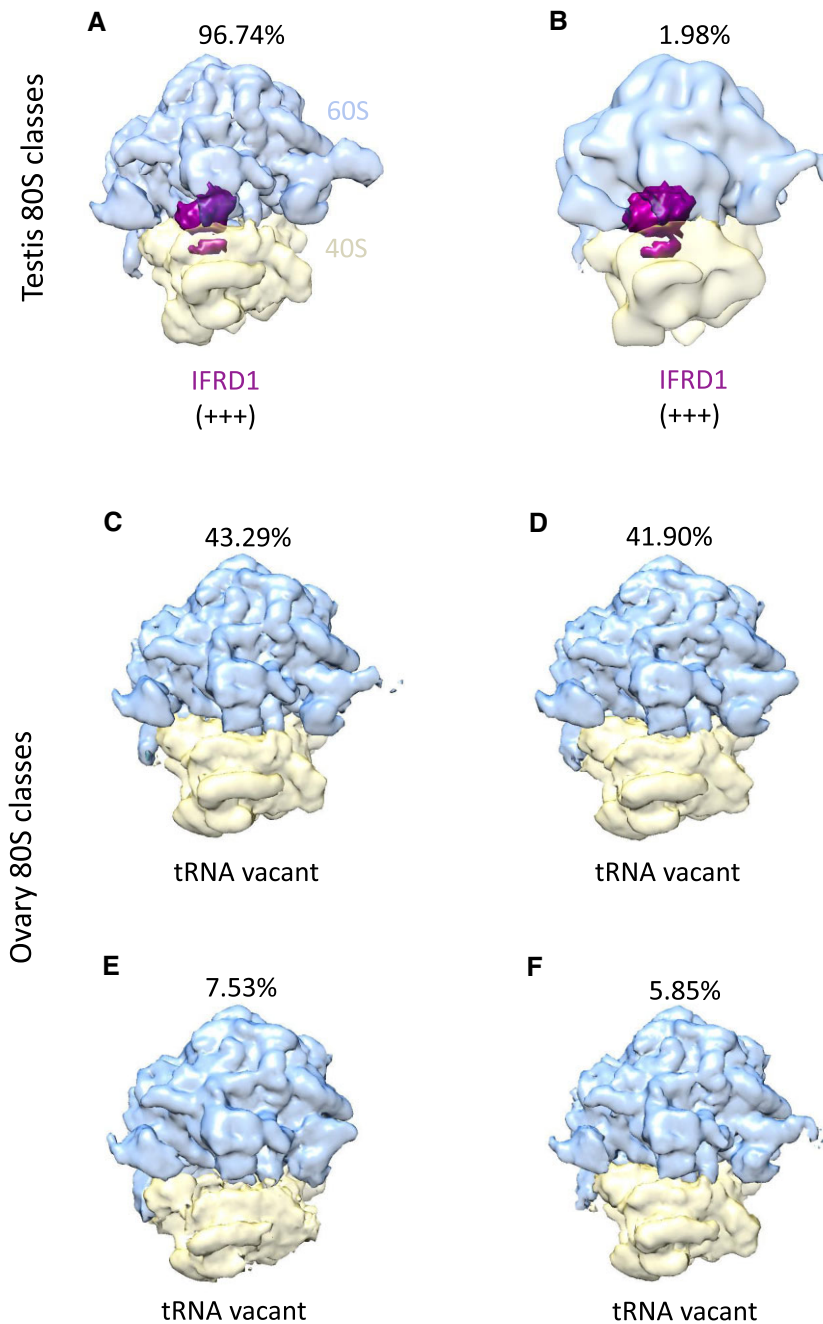


Figure 2. Testis and ovary 80S monosomes are not actively translating. Significant 3D classes (>1% total particles in dataset and >300 particles) of the testis 80S dataset (A and B) from ~47 000 particles; and ovary 80S dataset (C-F) from ~186 000 particles. (A and B) 2 classes of the testis 80S dataset, representing 96.74% and 1.98% of all testis 80S particles, contained a strong IFRD1 (purple) density in the mRNA channel. (C-F) All four significant classes from the ovary 80S dataset, representing 43.29%, 41.90%, 7.53%, and 5.85%, lacked tRNA at the mRNA channel. Percentage of particles in each class is given above each class. IFRD1 position is indicated along with score of confidence with +++ representing high confidence.

Head 80S monosomes and polysomes translate different mRNA pools

Given head 80S monosomes are engaged in active translation we sought to determine, which mRNAs they translate and if they differ from the mRNAs translated by polysomes. RNA-Seq was performed followed by DE analysis on RNAs bound by 80S ribosomes or polysomes compared to total cytoplasmic RNA (Fig. 5A). Principle Component Analysis (PCA) showed that replicates from these different subcellular fractions clustered together but represented distinct RNA populations to the other samples (Supplementary Fig. S7A). Around

784 genes were found to be preferentially translated by head 80S monosomes and 788 preferentially translated by head polysomes (adjusted P -value < 0.01) (Fig. 5B). GO term analysis on these enriched mRNA populations revealed that mRNAs preferentially translated by monosomes were enriched for mRNAs encoding the translational machinery (Fig. 5C). While polysome-translated mRNAs were enriched for mRNAs encoding proteins involved with neural function (Fig. 5D). This list of head monosome-enriched genes included 74 ribosomal proteins, 17 eIFs, 6 eEFs, RACK1, Poly A Binding Protein (PABP), and translationally controlled tumor protein

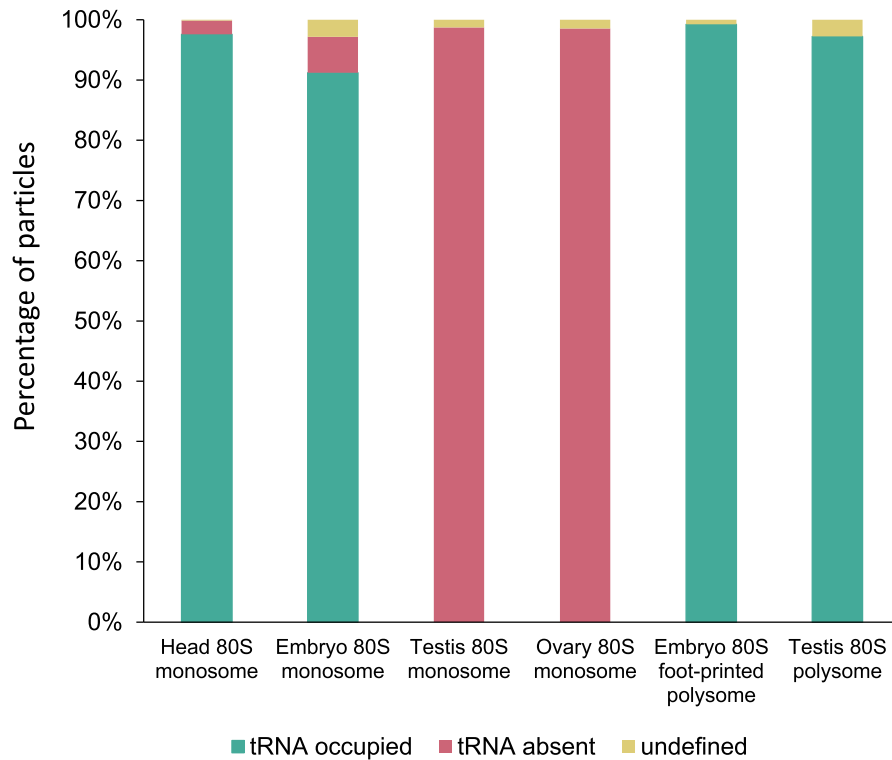


Figure 3. tRNA occupancy levels vary substantially across tissues. Bar chart showing percentages of particles for each dataset which either have tRNA densities present, absent, or resolution prevents definition (undefined).

(tctp). The mRNAs encoding these proteins have been previously shown to contain pyrimidine-containing TOP motifs, which are highly conserved between human and *Drosophila* [33]. Therefore, we analysed the 5'-UTR sequences of the 80S monosome enriched mRNAs, searching for overrepresented motifs. The most enriched motif, found in 15% of these mRNAs was the TOP motif (Fig. 5E and Supplementary Fig. S7B), whereas there were no overrepresented motifs in polysome enriched mRNAs. By analysing the attributes of the mRNAs preferentially translated by head 80S monosomes and polysomes, we discovered that monosome-translated mRNAs had significantly shorter ORFs (Fig. 5F), shorter 5'-UTRs (Fig. 5G) and shorter 3'-UTRs (Supplementary Fig. S7C). Monosome-translated mRNAs were also more likely to contain uORFs compared to polysomes-translated mRNAs (one-sided Fisher Exact Test P -value = 0.001645). Out of these attributes, CDS length is the one that contributes the most to the mRNA enrichment in monosomes (Supplementary Fig. S7D). Overall, these results show that head 80S and head polysomes translate different populations of mRNAs.

Discussion

The view that 80S monosomes represent lowly translating ribosomal complexes is mostly derived from tissue cultured cells. However, this has not been fully characterised *in vivo*. To test this, we purified and characterised 80S monosomes and polysomes from different *D. melanogaster* tissues. Our cryo-EM analysis revealed that substantial differences exist in the translational status of these 80S monosomes. The vast majority of 80S monosomes in the head (~98%) and embryo (~91%) contain tRNAs, indicating they are actively translat-

ing. While 80S monosomes in the testis are inactive by way of IFRD1 binding within the mRNA channel. This is in contrast to ovary 80S monosomes, which are vacant and can be disassociated with high KCl (200 mM). As expected, 80S particles from polysomes in both embryo and testis are occupied with tRNAs, therefore actively translating.

Danio rerio and *Xenopus laevis* eggs and embryos have been found to be bound by several dormancy factors [12]. Dap1b-eIF5a and Habp4-eEF2 act to stabilise 80S monosomes in eggs, repressing translation, ready for activation after fertilisation [12]. This is similar to our testis 80S monosomes, which have IFRD1 blocking the mRNA channel, and to IFRD2-inhibited ribosomes from rabbit reticulocyte lysate [13]. While our *Drosophila* embryos (0–2 h) represent a stage where translational repression has been relieved, similar to 3 h post-fertilisation in [12]. Therefore, we did not find evidence of any 80S monosome dormancy in 0–2 h *Drosophila* embryos, similar to previous cryo-EM of *D. melanogaster* 0–16 h [34] embryo 80S monosomes, which showed tRNA occupancy and no dormancy factors [35]. In the *Drosophila* ovary, there may be additional factors inhibiting translation via an alternative mechanism that does not involve blocking the tRNA sites.

The fact that 80S monosomes in embryos are the majority of the actively translating ribosomal complexes is consistent with the high levels of translation of uORFs in 0–2 h embryos detected by Ribo-Seq [6]. Given the small size of uORFs and therefore limited space for ribosomes to bind, only single 80S are expected to be translating at any one time. During early embryogenesis, when transcription is silent, translational control is essential and uORF translation is a widespread mechanism of translational repression of main ORFs in maternal mRNAs at this time [36].

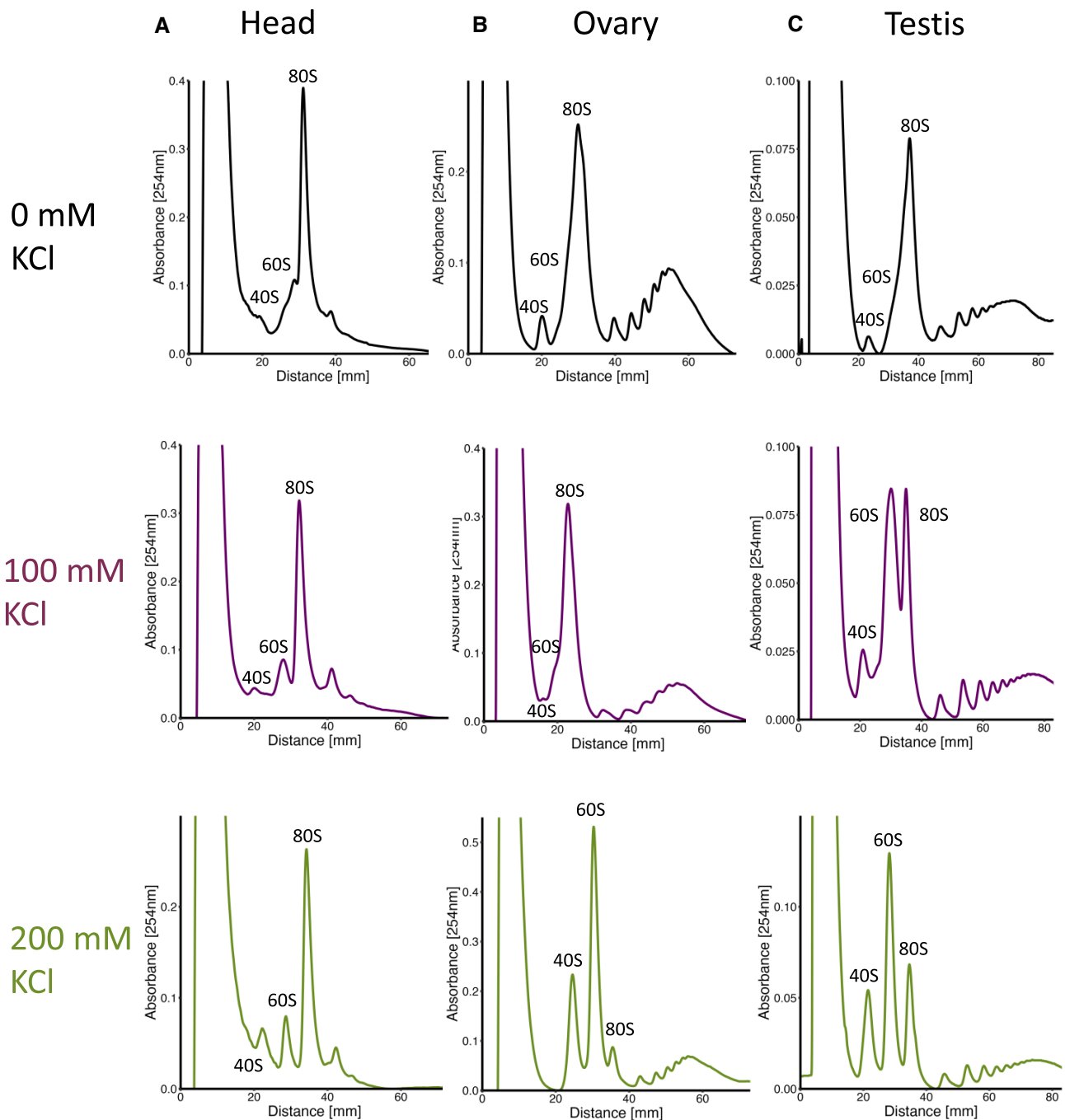


Figure 4. Differing KCl sensitivity of 80S monosome complexes. Sucrose gradient profiles at different KCl concentrations; 0 (black), 100 (purple), and 200 mM (green), ribosomal complexes indicated (40S, 60S, and 80S) for (A) head, (B) ovary, and (C) testis. Representative profiles are shown.

To determine the translational contribution of 80S monosomes in the head compared to polysomes we performed RNA-Seq. This showed that these two types of translational complexes have different translational preferences. Specifically, head polysomes preferentially translate mRNAs with neuronal functions. Whilst head 80S monosomes preferentially translate mRNAs encoding the translational machinery itself. These 80S monosome translated mRNAs contain TOP motifs, have short 5'-UTRs, contain short ORFs and are enriched for the presence of uORFs. Again, given that there is limited room on short ORFs and uORFs for ribosomes, our result fits with this restriction [6]. This is also consistent with

ribosome profiling of monosomes in *Saccharomyces cerevisiae* where most monosomes are actively elongating, and translate short ORFs, uORFs, NMD targets and low-abundance regulatory proteins [4].

Head 80S monosome-translated mRNAs also tend to have shorter 5'-UTRs and 3'-UTRs not just compared to polysome-translated but also shorter compared to all invertebrate transcripts [37]. The translational regulation of 5'TOP mRNAs has been shown to involve a shift in their translation between polysomes and monosomes [38]. In response to stresses such as starvation in tissue culture cells, the RNA-binding protein LARP1 represses 5'TOP mRNA translation, but basal levels

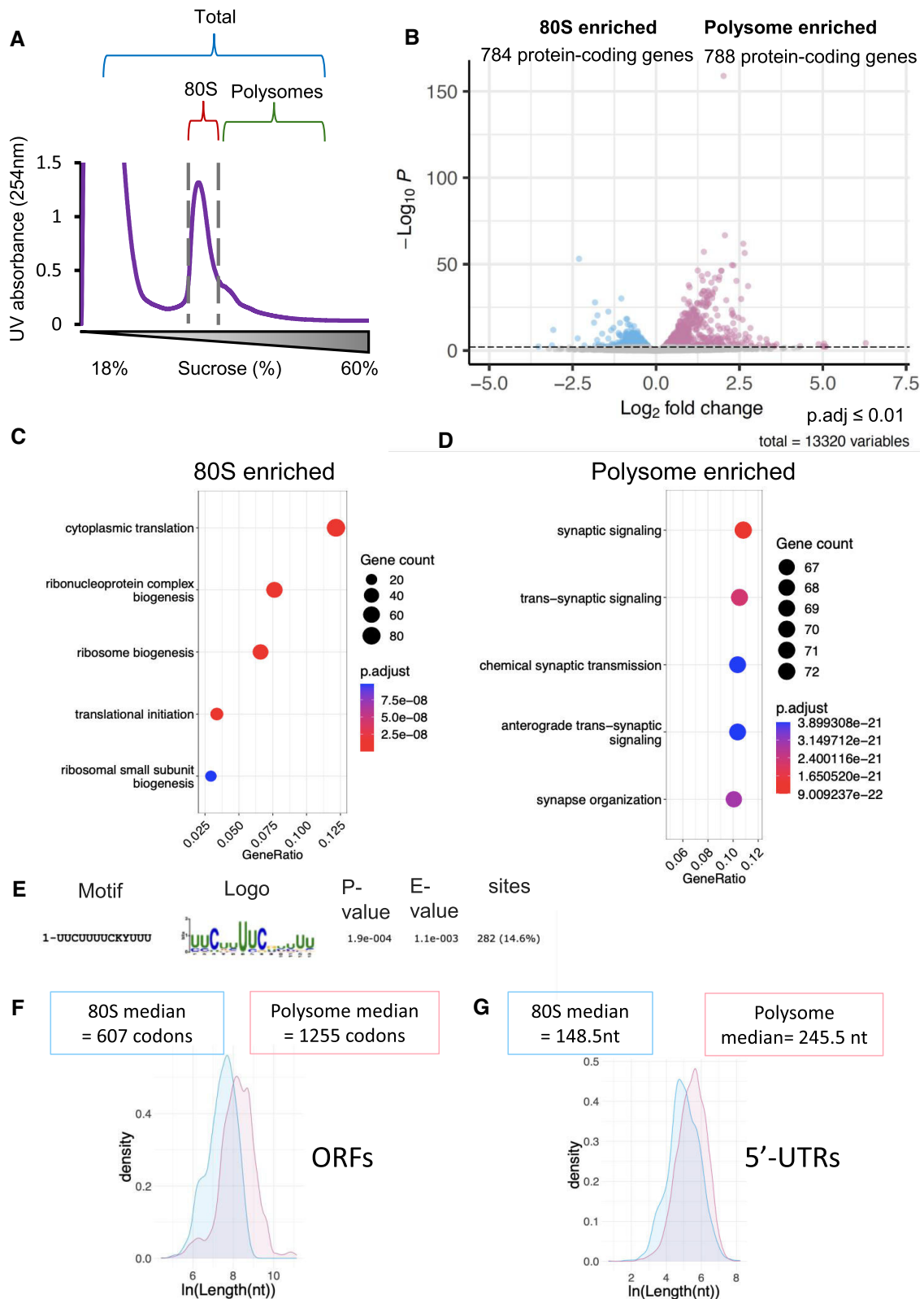


Figure 5. Head 80S monosomes and polysomes translate distinct mRNA populations. **(A)** Schematic of RNA-Seq samples from head ribosomal complexes. **(B)** Volcano plot of differentially enriched mRNAs between 80S monosomes (784) and polysomes (788) with a FDR < 0.01 threshold (dotted line). Over-represented GO terms found in **(C)** 80S monosome enriched mRNAs and **(D)** polysome-enriched mRNAs. **(E)** Most enriched motif in the 5'-UTRs of 80S monosome enriched mRNAs. Distributions of **(F)** ORF length (one-sided KS Test P -value = $4.5e^{-167}$) and **(G)** 5'-UTR length (one-sided KS Test P -value = $7.2e^{-56}$)(\ln of length in nt) for 80S monosome and polysome enriched transcripts, with medians provided (80S monosome; blue, polysome; pink).

of translation continue to occur by 80S monosomes. In mammalian systems, the mechanism for LARP1 has recently been revealed to include binding to free 40S subunits to achieve TOP mRNA repression [39]. Our heads come from well fed *D. melanogaster*, so starvation is unlikely to be the signal for our ribosomes, but a comparable regulatory network may exist in the head.

Our evidence for translation of neuronal function mRNAs by head polysomes may seem in contrast to previous evidence, indicating 80S monosomes actively translate synaptic mRNAs in neuronal processes [10]. However, we have isolated ribosomes from the whole fly head, only a proportion of which is brain. Therefore, our 80S monosomes could come from a variety of cell types in addition to neurons, such as glial cells, fat bodies and muscles. In fact, Ribo-Seq in *Drosophila* glia has revealed a substantial amount of uORF translation [40], which is likely contributing to 80S monosome translation in our analysis. Comparison of Ribo-Seq from glial cells and neurons indicates translational control is substantially different, and our analysis of whole heads will contain both types of translation events, along with the multiple other cell types, making direct comparison with neurons alone complex [10].

Overall, our results reveal that the translational status of 80S monosomes varies substantially across tissues, where these ribosomes represent the dominant translational complex compared to tissue culture cells.

Acknowledgements

We thank the Astbury Biostructure Laboratory (ABSL) Electron Microscopy Facility staff for assisting with cryo-EM data collection. We thank the Next Generation Sequencing facility, at St James University Hospital, Leeds, UK for performing Next Generation Sequencing. Parts of this work were undertaken on ARC3, part of the High Performance Computing facilities at the University of Leeds, UK. We thank Dr Tobias Schmidt and Dr Joe Waldron, CRUK Scotland Institute for gradient boosting code. The graphical abstract was created in BioRender. Aspden, J. (2025) <https://BioRender.com/36z35zm>.

Author contributions: A.B. performed experiments and analysed the data. T.H. conceived, designed, and performed experiments for this study and interpreted data. E.V., A.T., B.F., and M.A. performed experiments for this study and analysed the data. J.F. and J.L.A. conceived the work, designed the experiments, and interpreted the data. All authors contributed to manuscript writing, revision, and have approved the submitted version.

Supplementary data

Supplementary data is available at NAR online.

Conflict of interest

None declared.

Funding

A.B. and M.A. were funded from BBSRC DTP, BB/M011151/1. AT was funded by Wellcome Trust 102174/B/13/Z. T.H., J.F., and J.A. were funded by BBSRC grant BB/S007407/1 and BBSRC BB/X003086/1. BF

was funded by BB/X003086/1. Funding to pay the Open Access publication charges for this article was provided by Leeds University.

Data availability

RNA-Seq data have been deposited at Gene Expression Omnibus, GEO GSE267425. Cryo-EM data have been deposited at EMDB as detailed in Supplementary Table 1. (1) *Drosophila melanogaster* Head 80S biological replicate 1: global average, with P/E, P/P and A/A tRNAs (EMD-50827); class averages with P/P and A/A tRNAs (EMD-50821, EMD-50822 and EMD-50823); class average with P/E and A/P tRNAs (EMD-50824); class average with P/P tRNA (EMD-50825); vacant class average (EMD-50826). (2) *Drosophila melanogaster* Head 80S biological replicate 2: class average with P/E and A/P tRNAs (EMD-50830); class average with P/P tRNA (EMD-50831). (3) *Drosophila melanogaster* Testis 80S, based on EMD-10622: class averages with IFRD1 (EMD-50763 and EMD-50762). (4) *Drosophila melanogaster* Testis Polysomes, based on EMD-10623: class average with P/P and A/A tRNAs (EMD-50764). (5) *Drosophila melanogaster* Ovaries 80S, based on EMD-10624: vacant class averages (EMD-50765, EMD-50766, EMD-50767, and EMD-50768). (6) *Drosophila melanogaster* Embryo 80S: class averages containing tRNA (EMD-50769 and EMD-50770); vacant class average (EMD-50771); class average with E/E and P/P tRNAs (EMD-50772). (7) *Drosophila melanogaster* Embryo Polysome: class average with P/E and A/P tRNAs (EMD-50797); class average containing tRNA: (EMD-50798); class average with P/P and A/A tRNAs (EMD-50799); class average with E/E and P/P tRNAs (EMD-50800).

References

- Kong J, Lasko P. Translational control in cellular and developmental processes. *Nat Rev Genet* 2012;13:383–94. <https://doi.org/10.1038/nrg3184>
- Hinnebusch AG, Ivanov IP, Sonenberg N. Translational control by 5'-untranslated regions of eukaryotic mRNAs. *Science* 2016;352:1413–6. <https://doi.org/10.1126/science.aad9868>
- Warner JR, Knopf PM, Rich A. A multiple ribosomal structure in protein synthesis. *Proc Natl Acad Sci* 1963;49:122–9. <https://doi.org/10.1073/pnas.49.1.122>
- Heyer EE, Moore MJ. Redefining the translational status of 80S monosomes. *Cell* 2016;164:757–69. <https://doi.org/10.1016/j.cell.2016.01.003>
- Aspden JL, Eyre-Walker YC, Phillips RJ *et al*. Extensive translation of small open reading frames revealed by Poly-Ribo-Seq. *eLife* 2014;3:e03528. <https://doi.org/10.7554/eLife.03528>
- Arava Y, Wang Y, Storey JD *et al*. Genome-wide analysis of mRNA translation profiles in *Saccharomyces cerevisiae*. *Proc Natl Acad Sci* 2003;100:3889–94. <https://doi.org/10.1073/pnas.0635171100>
- Douka K, Birds I, Wang D *et al*. Cytoplasmic long noncoding RNAs are differentially regulated and translated during human neuronal differentiation. *RNA* 2021;27:1082–101. <https://doi.org/10.1261/rna.078782.121>
- Chassé H *et al*. Analysis of translation using polysome profiling. *Nucleic Acids Res* 2017;45:e15.
- Noll M, Hapke B, Schreier MH *et al*. Structural dynamics of bacterial ribosomes: I. Characterization of vacant couples and their relation to complexed ribosomes. *J Mol Biol* 1973;75:281–94. [https://doi.org/10.1016/0022-2836\(73\)90021-1](https://doi.org/10.1016/0022-2836(73)90021-1)

10. Biever A, Glock C, Tushev G *et al.* Monosomes actively translate synaptic mRNAs in neuronal processes. *Science* 2020;367:eaay4991. <https://doi.org/10.1126/science.aay4991>
11. Helena-Bueno K, Rybak MY, Ekemezie CL *et al.* A new family of bacterial ribosome hibernation factors. *Nature* 2024;626:1125–32. <https://doi.org/10.1038/s41586-024-07041-8>
12. Leesch F, Lorenzo-Orts L, Pribitzer C *et al.* A molecular network of conserved factors keeps ribosomes dormant in the egg. *Nature* 2023;613:712–20. <https://doi.org/10.1038/s41586-022-05623-y>
13. Brown A, Baird MR, Yip MC *et al.* Structures of translationally inactive mammalian ribosomes. *eLife* 2018;7:e40486. <https://doi.org/10.7554/eLife.40486>
14. Hopes T, Norris K, Agapiou M *et al.* Ribosome heterogeneity in *Drosophila melanogaster* gonads through paralogue-switching. *Nucleic Acids Res* 2022;50:2240–57. <https://doi.org/10.1093/nar/gkab606>
15. Thompson RF, Iadanza MG, Hesketh EL *et al.* Collection, pre-processing and on-the-fly analysis of data for high-resolution, single-particle cryo-electron microscopy. *Nat Protoc* 2019;14:100–18. <https://doi.org/10.1038/s41596-018-0084-8>
16. Zivanov J, Nakane T, Forsberg BO *et al.* New tools for automated high-resolution cryo-EM structure determination in RELION-3. *eLife* 2018;7:e42166. <https://doi.org/10.7554/eLife.42166>
17. Zhang K. Gctf: real-time CTF determination and correction. *J Struct Biol* 2016;193:1–12. <https://doi.org/10.1016/j.jsb.2015.11.003>
18. Li X, Mooney P, Zheng S *et al.* Electron counting and beam-induced motion correction enable near-atomic-resolution single-particle cryo-EM. *Nat Methods* 2013;10:584–90. <https://doi.org/10.1038/nmeth.2472>
19. Wagner T, Merino F, Stabrin M *et al.* SPHIRE-crYOLO is a fast and accurate fully automated particle picker for cryo-EM. *Commun Biol* 2019;2:218. <https://doi.org/10.1038/s42003-019-0437-z>
20. Ewels P, Magnusson M, Lundin S *et al.* MultiQC: summarize analysis results for multiple tools and samples in a single report. *Bioinformatics* 2016;32:3047–8. <https://doi.org/10.1093/bioinformatics/btw354>
21. Bolger AM, Lohse M, Usadel B. Trimmomatic: a flexible trimmer for Illumina sequence data. *Bioinformatics* 2014;30:2114–20. <https://doi.org/10.1093/bioinformatics/btu170>
22. Dobin A, Davis CA, Schlesinger F *et al.* STAR: ultrafast universal RNA-seq aligner. *Bioinformatics* 2013;29:15–21. <https://doi.org/10.1093/bioinformatics/bts635>
23. Liao Y, Smyth GK, Shi W. featureCounts: an efficient general purpose program for assigning sequence reads to genomic features. *Bioinformatics* 2014;30:923–30. <https://doi.org/10.1093/bioinformatics/btt656>
24. Love MI, Huber W, Anders S. Moderated estimation of fold change and dispersion for RNA-seq data with DESeq2. *Genome Biol* 2014;15:550. <https://doi.org/10.1186/s13059-014-0550-8>
25. Wu T *et al.* clusterProfiler 4.0: a universal enrichment tool for interpreting omics data. *Innovation (Camb)* 2021;2:100141.
26. Bailey TL, Johnson J, Grant CE *et al.* The MEME Suite. *Nucleic Acids Res* 2015;43:W39–49. <https://doi.org/10.1093/nar/gkv416>
27. Patraquim P, Mumtaz MAS, Pueyo JI *et al.* Developmental regulation of canonical and small ORF translation from mRNAs. *Genome Biol* 2020;21:128. <https://doi.org/10.1186/s13059-020-02011-5>
28. Aspden JL, Jackson RJ. Differential effects of nucleotide analogs on scanning-dependent initiation and elongation of mammalian mRNA translation *in vitro*. *RNA* 2010;16:1130–7. <https://doi.org/10.1261/rna.1978610>
29. Sinha NK, Ordureau A, Best K *et al.* EDF1 coordinates cellular responses to ribosome collisions. *eLife* 2020;9:e58828. <https://doi.org/10.7554/eLife.58828>
30. Martin TE, Hartwell LH. Resistance of active yeast ribosomes to dissociation by KCl. *J Biol Chem* 1970;245:1504–6. [https://doi.org/10.1016/S0021-9258\(18\)63264-8](https://doi.org/10.1016/S0021-9258(18)63264-8)
31. Infante AA, Baierlein R. Pressure-induced dissociation of sedimenting ribosomes: effect on sedimentation patterns. *Proc Natl Acad Sci* 1971;68:1780–5. <https://doi.org/10.1073/pnas.68.8.1780>
32. Saba JA *et al.* LARP1 senses free ribosomes to coordinate supply and demand of ribosomal proteins. bioRxiv, <https://doi.org/10.1101/2023.11.01.565189>, 2 November 2023, preprint: not peer reviewed.
33. Meyuhis O, Dreazen A. Ribosomal protein S6 kinase from TOP mRNAs to cell size. *Prog Mol Biol Transl Sci* 2009;90:109–53. [https://doi.org/10.1016/S1877-1173\(09\)90003-5](https://doi.org/10.1016/S1877-1173(09)90003-5)
34. Gebauer F, Corona DF, Preiss T, Becker PB, Hentze MW. Translational control of dosage compensation in *Drosophila* by Sex-lethal: cooperative silencing via the 5' and 3' UTRs of msl-2 mRNA is independent of the poly(A) tail. *EMBO J* 1999;18:6146–54. <https://doi.org/10.1093/emboj/18.21.6146>
35. Anger AM, Armache J-P, Berninghausen O *et al.* Structures of the human and *Drosophila* 80S ribosome. *Nature* 2013;497:80–5. <https://doi.org/10.1038/nature12104>
36. Dunn JG, Foo CK, Belletier NG *et al.* Ribosome profiling reveals pervasive and regulated stop codon readthrough in *Drosophila melanogaster*. *eLife* 2013;2:e01179. <https://doi.org/10.7554/eLife.01179>
37. Mignone F, Gissi C, Liuni S *et al.* Untranslated regions of mRNAs. *Genome Biol* 2002;3:reviews0004.1. <https://doi.org/10.1186/gb-2002-3-3-reviews0004>
38. Schneider C, Erhard F, Binotti B *et al.* An unusual mode of baseline translation adjusts cellular protein synthesis capacity to metabolic needs. *Cell Rep* 2022;41:111467. <https://doi.org/10.1016/j.celrep.2022.111467>
39. Saba JA, Huang Z, Schole KL *et al.* LARP1 binds ribosomes and TOP mRNAs in repressed complexes. *EMBO J* 2024;43:6555–72. <https://doi.org/10.1038/s44318-024-00294-z>
40. Ichinose T, Kondo S, Kanno M *et al.* Translational regulation enhances distinction of cell types in the nervous system. *eLife* 2023;12:RP90713. <https://doi.org/10.7554/eLife.90713.2>